www.sciencemag.org/content/359/6383/1520/suppl/DC1

Supplementary Materials for

Erythrocytic ferroportin reduces intracellular iron accumulation, hemolysis, and malaria risk

De-Liang Zhang, Jian Wu, Binal N. Shah, Katja C. Greutélaers, Manik C. Ghosh, Hayden Ollivierre, Xin-zhuan Su, Philip E. Thuma, George Bedu-Addo, Frank P. Mockenhaupt, Victor R. Gordeuk, Tracey A. Rouault*

*Corresponding author: Email: rouault@mail.nih.gov

Published 30 March 2018, *Science* **359**, 1520 (2018)
DOI: 10.1126/science.aal2022

This PDF file includes:

Other Supporting Online Material for this manuscript includes the following:
(available at www.sciencemag.org/content/359/6383/1520/suppl/DC1)

Table S1 (Excel)

SUPPLEMENTARY MATERIALS

Materials and Methods

Human Study

RBC ghost membrane preparation: The human red blood cells were isolated from the de-identified buffy coats from healthy volunteer donors from the Department of Transfusion Medicine, NIH Clinical Center, and the majority of the Buffy coat was RBCs, and a small percentage was white blood cells. Briefly, one mL of Buffy coat was centrifuged for 5 min at 3000g at 4^{o}C. After removing the plasma and white blood cells, the RBCs were washed for three times with ice-cold PBS, before being lysed in 10 volumes of 5 mM sodium phosphate buffer, pH8.0. The RBC ghosts were pelleted by centrifugation at 10000g for 5 min at 4^{o}C, and washed with 5mM sodium phosphate buffer for three times, and then lysed in 5 volumes of RIPA buffer (50 mM Tris pH7.4, 150 mM NaCl, 0.1% SDS, 0.5% Na.Deoxycholate, 1% Triton X-100, 5mM EDTA, Halt protease inhibitor). ***FPN Q248H mutation genotyping of African-American blood donors:*** *FPN Q248H* mutation was genotyped accordingly to the method described previously with PCR and subsequent *Pvu II* endonuclease digestion (*29*). ***RBCs from Sickle cell disease*****:** The RBCs of Sickle Cell Disease were isolated from de-identified whole blood donated by SCD patients and provided by Dr. John Tisdale. The samples were centrifuged at 3000g for 5 min to separate plasma, white blood cells and RBCs. The plasma was removed for ferritin determination, and after removing white blood cells, RBC membrane fractions were prepared as above described.

FPN Q248H mutation in Zambian malaria patients: The cohort of malaria patients in Zambia has been described previously (*32*). The study was approved by the Research Ethics Committee of the University of Zambia, and written informed consent was obtained for each participant. Sample collection was longitudinal as patients presented to the hospital and the parents agreed for study participation. For determination of *FPN Q248H*, genomic DNA was isolated from dried blood spots on filter paper. Briefly, strips of filter paper were washed for 2 hours with 200 µL of Qiagen generation DNA Purification Solution 1, followed by a 30-min wash with 150 µL of generation DNA Elution Solution 2 at room temperature. DNA was eluted from the paper by heating at 99°C for 15 minutes in 60 µl of DNA Elution Solution 2 in a thermal cycler. The crude DNA lysate was used for genotyping for *Q248H* using a TaqMan SNP genotyping assay (C_25753769_10, Life Technologies) in combination with GTXpress Master Mix (Applied Biosystems), in a StepOnePlus™ Real-Time PCR System (Applied Biosystems). Allelic discrimination calls were made using Step one software v2.3.

FPN Q248H mutation in Ghanaian pregnant women: The characteristics of a total of 889 delivering women attending the Presbyterian Mission Hospital in Agogo, Ghana, in 2000 to 2001 have been reported previously (*37*). The study was reviewed and approved by the Committee on Human Research, Publication and Ethics of the Kwame Nkrumah University of Science and Technology, Kumasi, and informed written consent was obtained from all study participants. Samples were collected subsequently throughout a year. Briefly, peripheral venous and placental (intervillous) blood was collected into EDTA-coated tubes. Malaria parasites were counted microscopically on Giemsa-stained thick blood films *per* 500 white blood cells for peripheral samples and *per* 100 high-power fields for placental samples, in which the presence of leukocyte-associated hemozoin (malaria pigment) was also recorded. Following DNA extraction (QIAamp, Qiagen, Germany), nested *P. falciparum*-specific PCR assays were performed (*38*). Present or past placental *P. falciparum* infection was defined as the presence of placental parasitemia or hemozoin by microscopy, or a positive *P. falciparum* PCR result on placental samples. Low birth weight (<2500 g) and preterm delivery (<27 gestational weeks) were assessed within 24 hours after delivery; hemoglobin was measured using a HemoCue (Angelholm, Sweden) photometer and anemia defined as Hb<11g/dL. For the present analysis, 290 of 304 primiparous women with live singleton delivery were successfully genotyped for the FPN Q248H mutation by PCR-RFLP in individual, single tube PCR assays (*39*).

Mice

All the mouse experiments were done following protocols approved by the Animal Care and Use Committee of NICHD and NIAID, and met NIH guidelines for the humane care of animals. $Fpn^{fl/fl}$ and $ErCre^{+/-}$ mice were described previously (*14, 20*) and were gifts from Dr. Nancy Andrews and Dr. Stuart Orkin, respectively. The $Fpn^{fl/fl}$ mice have a 129/SvEvTac background; the $ErCre^{+/-}$ mice have a BALB/c background; and siblings were used in all experiments to minimize background difference. The mice were genotyped by PCR according to the original description. The mice were weaned at 3-4 weeks age and maintained on the normal NIH-07 diet (350 mg iron/kg) manufactured by Harlan Teklad. For the high and low iron diet experiments, the mice were maintained on a high-iron diet (1.6 g iron/kg) or low-iron diet (2-6 mg iron/kg) (Harlan Teklad) for at least 3 months since weaning before doing the experiment. All the experiments were done with 3-6 months old mice except otherwise mentioned.

Blood indices

Blood of 50 μL was collected from facial vein to heparin-coated tube and then was analyzed with IDEXX ProCyte Dx Hematology Analyzer.

Malaria infection, parasitemia and survival curve

To test the effect of FPN abundance on malaria infection, 4-5 months old male mice were injected intravenously with 1x10e6 RBCs infected with *Plasmodium Yoelii YM* parasites or *Plasmodium chabaudi chabaudi AS.* The parasitemia and survival of the mice were monitored daily. To check parasitemia with Giemsa staining, one drop of blood was collected to prepare a blood smear that was then stained with Giemsa staining. Parasite-positive cells were counted under a microscope. For counting parasitemia with flow cytometry, 1 μL blood in 100 μL PBE buffer (1% bovine serum albumin, 2 mM EDTA in PBS buffer) was incubated with 0.25X SYBR Green I and 0.5 μM of SYTO61 for 30 min at room temperature on a shaker. Then the sample was diluted with 400 μL of cold PBS on ice and analyzed using BD FACSAria II flow cytometer within an hour. The procedures of infecting mice with *P. yoelii* YM and *P. chabaudi* parasite were performed in accordance with the approved protocol (approval #LMVR11E) by Institutional Animal Care and Use Committees (IACUC) at the National Institute of Allergy and Infectious Diseases (NIAID) following the guidelines of the Public Health Service Policy on Humane Care and Use of Laboratory Animals and AAALAC.

ELISA to measure Epo, haptoglobin and ferritin

ELISA kits were used to measure EPO (R&D Systems), haptoglobin (Life Diagnostics), and ferritin (Abcam) levels according to manufacturer's protocols.

Non-heme Iron and labile iron pool measurement

Non-heme iron was measured according to the previous description (*34*). **Labile iron pool (LIP)** was measured according to the previous description with modification (*40*). Briefly, 20 μL blood collected with heparin-coated tube was washed twice with PBS, and then was incubated with 250 nM calcein/AM in 154 mM NaCl, 20 mM HEPES, 5 mM glucose, pH 7.35 with or without 100 μM salicylaldehyde isonicotinoyl hydrazone (SIH) for 30min at 37°C with constant shaking. After washing with cold PBS for twice, fluorescence was measured by flow cytometry on FITC channel with FACSAria flow cytometer for 100,000 RBCs. The LIP is calculated by subtracting the MFI (median fluorescence intensity) of the sample without SIH from the MFI of the sample treated with SIH.

ROS measurement

Blood was washed twice in PBS and then 2x10e6 cells in 100 μL PBS were incubated with 10 μL H2DCFDA (Thermo Fisher Scientific) with or without 10, 20 or 50 μL H_2O_2 for 15min at 37°C on a shaker. After washing twice with cold PBS, the fluorescence was measured with a FACSAria flow cytometer.

Osmotic fragility assay

The osmotic fragility of RBCs was measured according to literature protocols with minor modifications (*41*). Briefly, 5 μL of blood collected in a heparin-coated tube was added to 200 μL of different concentration of NaCl solutions, incubated for 10min at RT, centrifuged at 3000g for 5 min, and then moved 150 μL supernatant into 96-well plate and measured the absorption at 540nm with a plate reader. The fragility curve was created by plotting NaCl concentration vs. percentage of hemolysis.

Isolation of bone marrow erythroblasts

Bone marrow erythroblasts were isolated with Dynabead® Biotin Binder (Thermo Fisher Scientific) with biotinylated Ter119 antibodies (R&D systems), respectively, according to our protocol described previously (*18*).

Hepcidin treatment

Bone marrow was flushed out from the mouse femur by syringe with a 25G needle with DMEM medium. After passing through a 10 mL pipette tip for 10 times, the bone marrow suspension was filtered through a 40 μm cell strainer to get single cells, and then was centrifuged at 500g for 3min to generate a cell pellet, which was then resuspended and cultured in StemPro-34 serum-free medium (Thermo Fisher Scientific) supplemented with 2 U/mL human recombinant erythropoietin, 100 ng/mL murine recombinant stem cell factor, 10 μM synthetic glucocorticoid dexamethasone, 40 ng/mL insulin-like growth factor 1, 2mM L-glutamine, 75 μg/mL human holo-transferrin, 140 mM monothioglycerol, 100 U/mL penicillin, and 100 μg/mL streptomycin at 37°C with 5% CO_2. After culturing for 24 hours, the cell suspension was moved to a 15-mL conical tube, all the attached cells including monocyte, macrophage, and stromal cells were discarded. After centrifugation at 500g for 3min, the cell pellet was resuspended in 2 mL of DMEM and separated by Ficoll to get rid of mature RBCs. Erythroblasts were then cultured in StemPro-34 medium with or without 1 μg/mL hepcidin (Bachem) for 24 hours. As for the RBCs treated with

hepcidin, blood was washed with DMEM for twice and then was cultured in StemPro-34 medium with or without hepcidin for 24 hours.

RBC lifespan and aging experiment

The RBC lifespan was measured with biotin labeling according to the previous description (*42, 43*). Briefly, 100 mg/kg body weight Sulfo-NHS-LC-Biotin (Thermo Fisher Scientific) in saline buffer was injected by tail vein. Blood of 20 μL was collected from the facial vein at different time points, and the percentage of biotinylated RBCs was checked with Cy3-anti-Biotin antibody by a FACSAria flow cytometer. **For the RBC aging experiment**, we labeled RBCs *in vivo* with Sulfo-NHS-LC-Biotin, collected blood at different subsequent time points, washed twice, and the Biotinylated RBCs were then purified with Dynabead® Biotin Binder, and then FPN levels were selectively assessed on a cohort of aging cells with Western blot. **For the in vitro Biotin labeling experiment** (fig. S9), blood from WT and *Fpn* KO mice was washed three times with PBS, and then labeled with Sulfo-NHS-LC-Biotin 10 μg/mL for *Fpn* KO blood or 30 μg/mL for WT blood at 37°C for 30 min with constant shaking. After washing with PBS for three times, *Fpn* KO and WT blood samples were mixed in a 1:1 ratio and adjusted to 1x10e7 cells/μL, and then injected (300 μL per mouse) via tail vein into WT mice. After 24 hours, 20 μL blood was collected and the percentage of Biotinylated RBCs was measured with Cy3-anti-Biotin antibody by a FACSAria flow cytometer.

RBC ghost membrane preparation

After centrifugation and removal of the buffy coat, RBCs were washed three times with cold PBS. RBC pellets were then lysed in 10 volume of 5 mM sodium phosphate buffer, pH8.0. The RBC ghosts were pelleted by centrifugation at 10,000g for 5 min at 4°C, washed with 5mM sodium phosphate buffer three times, and then lysed in 5 volumes of RIPA buffer for western blot analysis.

Human RBC mass spectrum data

The mass spectrum data for red cell membrane were reported by Pesciotta and her colleagues in their previous publication (*21*), and were downloaded from the Peptide Atlas data repository with the dataset identifier PASS00334 (www.peptideatlas.org). The data were analyzed with Excel, and the number of peptides identified for each protein was summarized and listed accordingly. The abundance of Band 3 was taken as 1000,000 copies per cell (*44*), and the rest of the proteins were normalized with Band 3 accordingly.

RT-PCR

Total RNAs were prepared with TRIzol® reagent (Ambion), 2 μg RNAs were then reversely transcribed into cDNA with High-Capacity cDNA Reverse Transcription kit (Applied Biosystems), and quantitative Real-Time PCRs were performed with Fast SYBR® Green PCR master mixture (Applied Biosystems) on a StepOnePlus™ Real-Time PCR System. The primers were shown in Supplemental table S5. The gene expressions were normalized against actin levels.

Western blot

Cells were lysed in 10 volumes of RIPA buffer (50 mM Tris pH7.4, 150 mM NaCl, 0.1% SDS, 0.5% Na.Deoxycholate, 1% Triton X-100, 5mM EDTA, Halt protease inhibitor) and then were centrifuged at 20,000g for 5min to generate protein lysates. The protein concentration was determined with Bradford method with Bio-Rad Protein Assay Dye Reagent (Bio-Rad) and then mixed with 2x loading buffer (50 mM Tris-HCl, pH 6.8, 2% SDS, 10% Glycerol, 1% b-Mercaptoethanol, 12.5 mM EDTA, 0.02 % Bromophenol Blue). The protein samples with loading buffer were incubated at 37°C for 15 min with antibodies to TfR1, FPN1, DMT1, or at 95°C for 5min for rest of the antibodies. After mixing and brief centrifugation, the samples were separated on 4-12% Bis-Tris gel (Thermo Fisher Scientific), and then transferred to nitrocellulose membrane. The membranes were blocked with 5% Non-fat milk in PBS with 0.1% Tween-20 for 30 min, and then incubated with primary antibodies overnight at 4°C. The blots were incubated with secondary antibodies for 1 hour at room temperature, and then developed on x-film with SuperSignal West Pico ECL substrates (Thermo Fisher Scientific). Primary antibodies: Rabbit anti-Mouse FPN antibody (MTP11-A, alpha-Diagnostics); Rabbit anti-FPN (ab85370, Abcam); Rabbit anti-FPN (NBP1-21502, Novus Biologicals); Mouse Monoclonal anti-β–Actin antibody (Sigma); Mouse Monoclonal anti-TfR1 antibody (Thermo Fisher Scientific); Rabbit anti-FPN MAP24 antibody, Rabbit anti-L-ferritin antibody, Rabbit anti-total DMT1 antibody, Rabbit anti-IRP1 antibody were developed in the lab and had been described previously (*18, 45, 46*). Molecular weight markers (kDa) were labeled on the right of the blots to indicate the size of the bands.

Flow Cytometry analysis and cell sorting

Bone marrow was flushed out with PBE buffer (1% bovine serum albumin, 2 mM EDTA in PBS buffer) by syringe with a 25G needle. The spleen was torn into small pieces with forceps in PBE buffer. The cell and tissue suspensions were then passed through a 10

mL pipette tip 10 times to separate into single cell suspensions, and filtered through a 40 μm cell strainer to generate single cell suspensions. To stain the cells, 1x10e6 cells were incubated with antibodies in 100 μL of PBE buffer for 30 min at 4°C on a shaker, and then diluted in 0.5 mL PBE buffer before being checked with Flow Cytometer. **For measuring different stages of erythroblasts**, cells were incubated with FITC-CD71 (BD Biosciences: 553266), PE-Cy7-Ter119 (BD Biosciences: 557853), 7-AAD (BD Bioscience: 559925), APC-Annexin V (BD Biosciences: 550474), APC-Cy7-CD45 (BD Biosciences: 557659), APC-Cy7-CD11b (BD Biosciences: 557657), APC-Cy7-Ly6g/6c (BD Biosciences: 557661), PE-CD44 (BD Biosciences: 553134). For analysis of different stages of erythroblasts, single cells were gated into 7-AAD negative cells, then were gated into CD45/CD11b/Ly6g/Ly6c negative cells, then were gated into Ter119 positive cells, which were then analyzed according to CD44 levels and cell size (FSC, Forward Scatter) (*36*). For analysis of cell population by CD71 and Ter119 staining, 7-AAD negative single cells were plotted by CD71 and Ter119 combination. **For analysis of Annexin V staining**, 7-AAD negative single cells were gated into different populations and then measured median fluorescence intensity of APC-Annexin V. **For bone marrow cell sorting**, single cell suspensions of bone marrow were incubated with 7-AAD, FITC-Ter119 (BD Biosciences: 557915) and APC-CD71 (eBioscience: 17-0711-82) to stain the cells, and then 2x10e6 cells were sorted into PBE buffer for cell lysate preparation with RIPA buffer. **For May-Grünwald-Giemsa staining**, sorted cells were attached to slide with Cytospin and then stained with May-Grünwald and Giemsa buffers (Sigma) according to manufacturer's protocol. All of the FACS analyses were measured by FACSAria II flow cytometer, and analyzed by FlowJo software.

RBC Iron-55 export assay

To measure the iron export activity of FPN, 0.2 mL RBC pellets from WT or *Fpn* KO mice were mixed and incubated with 20 μCi ^{55}FeCl3 (PerkinElmer) in 0.5 mL of ice-cold 5P8-1Mg buffer (1 mM MgSO4 in 5 mM sodium phosphate buffer, pH8.0) for 5 min on ice (*47*). During the incubation, RBCs would briefly lyse and then spontaneously reseal shortly after, to trap ^{55}Fe inside the RBCs and also preserve a significant amount of cytosolic proteins inside the cells, which ensured that the iron chaperones, if there were any, would be preserved inside RBCs. The samples were then spun down at 20,000g for 10 min at 4 °C to separate from the 5P8-1Mg buffer, and then were resuspended in 1 mL PBS followed by incubation at 37 °C for 5 min on a thermomixer to seal the RBCs. After washing with PBS at 1000g x 3min for 2 times, the samples were incubated at 37 °C for 5 min to seal the RBCs again followed by washing with PBS at 1000g x 3min for 3 more times. The

RBCs were then incubated in DMEM medium with 50% FBS for 1 hour at 37 ^{o}C, or at 4 ^{o}C, or at 37 ^{o}C with 1 μg/mL hepcidin. The high percentage of FBS ensures that there is enough apo-transferrin to accept iron exported by FPN, and also protects RBCs from auto-hemolysis. Then the ^{55}Fe in the medium was measured by liquid scintillation and the number was divided by the ^{55}Fe inside RBCs before the 1-hour incubation to calculate the percentage of ^{55}Fe exported by FPN.

Statistical analysis

For the Zambian human study, categorical variables were compared with the Fisher exact test and continuous variables were compared with the Kruskal-Wallis test. For the Ghanaian human study, the association of *FPN Q248H* mutation with malaria infection as a categorical variable was analyzed with Chi-Square Test, and odds ratios (ORs) and 95% confidence intervals (95% CIs) were calculated. The odds of infection in *FPN Q248H* carriers were adjusted for known predictors of placental malaria in this group by logistic regression. Continuous variables were compared between groups by Student´s t-test and presented as mean ± standard deviation, or by the non-parametric Mann-Whitney U-test and presented as median (range), as applicable. Potential interactions of *FPN* Q248H genotype and infection on clinical outcomes were assessed by analysis of variance (ANOVA).

For mouse studies, significances for two-group comparisons were determined using two-tailed Unpaired t-tests. Significances for two-group comparisons with apparently unequal variances were determined using Welch's t-test. Significances for multi-group comparisons were analyzed with one-way ANOVA followed by Tukey's multiple comparisons tests, or two-way ANOVA followed by Sidak's multiple comparisons test, or Holm-Sidak method with alpha = 0.05 at where appropriate. The survival curves were analyzed with Log-rank test and Gehan-Breslow-Wilcoxon test. All tests were performed with GraphPad Prism 7, and data were expressed as mean ± 95% confidence interval (CI) except where indicated otherwise. The data were taken as significant when p value<0.05 (*p<0.05, **p<0.01, ***p<0.001, ****p<0.0001).

Figure S1.

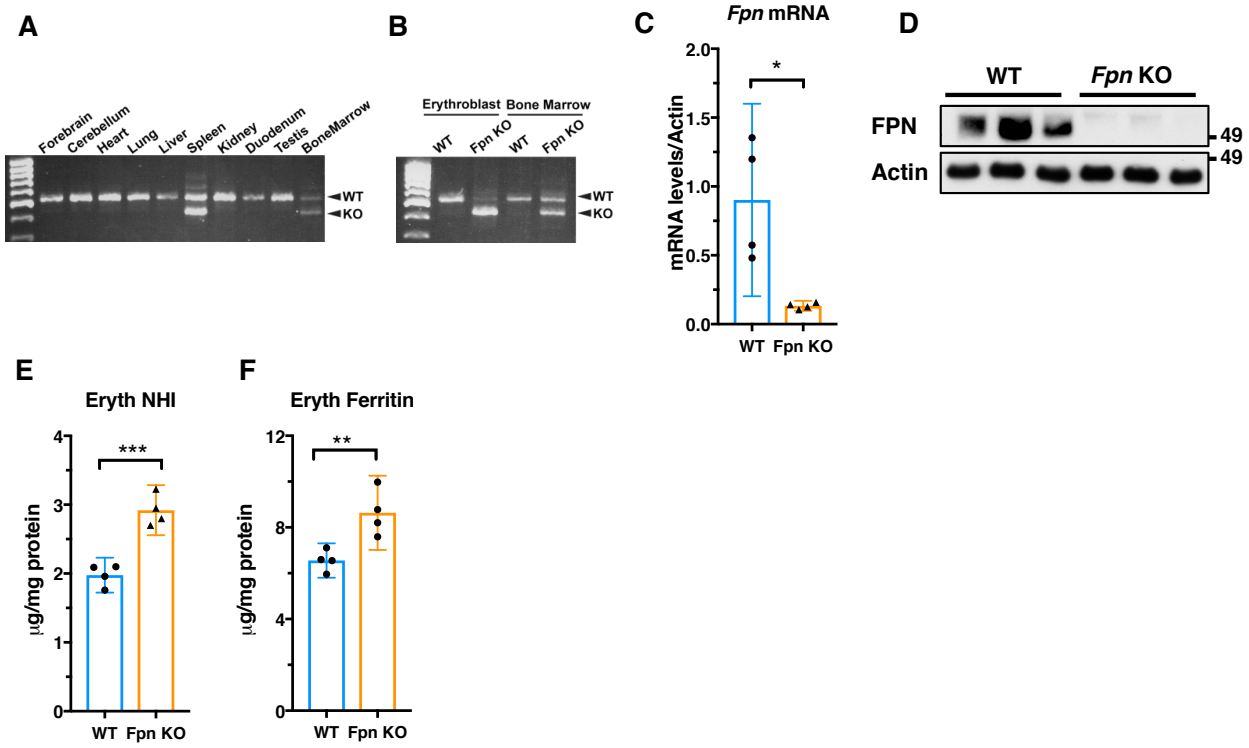

Figure S1. Cell-specific knockout of *Fpn* in erythroblasts caused cellular iron overload. (**A**) PCR with genomic DNA from different tissues of *Fpn*$^{fl/fl}$;*ErCre*$^{+/-}$ mice (*Fpn* KO) showed that the *Fpn* KO band (398bp) was present only in spleen and bone marrow, two erythropoietic tissues, in contrast to the ubiquitous expression of WT band (522bp). (**B**) WT and *Fpn* KO bands in total bone marrow and purified erythroblasts of WT and *Fpn* KO mice showed erythroblast-specific knockout of *Fpn.* (**C**) *Fpn* mRNA and (**D**) protein levels in the erythroblasts of WT and *Fpn* KO mice. (**E**) non-heme iron (NHI) and (**F**) ferritin levels in purified erythroblasts of WT and *Fpn* KO mice. Results showed that *Fpn* KO dramatically increased intracellular NHI and ferritin levels, indicating excess iron accumulated. Data are presented as Mean ± 95% confidence interval. Erythroblasts were purified with biotinylated Ter119 antibodies and Dynabead®.

Figure S2.

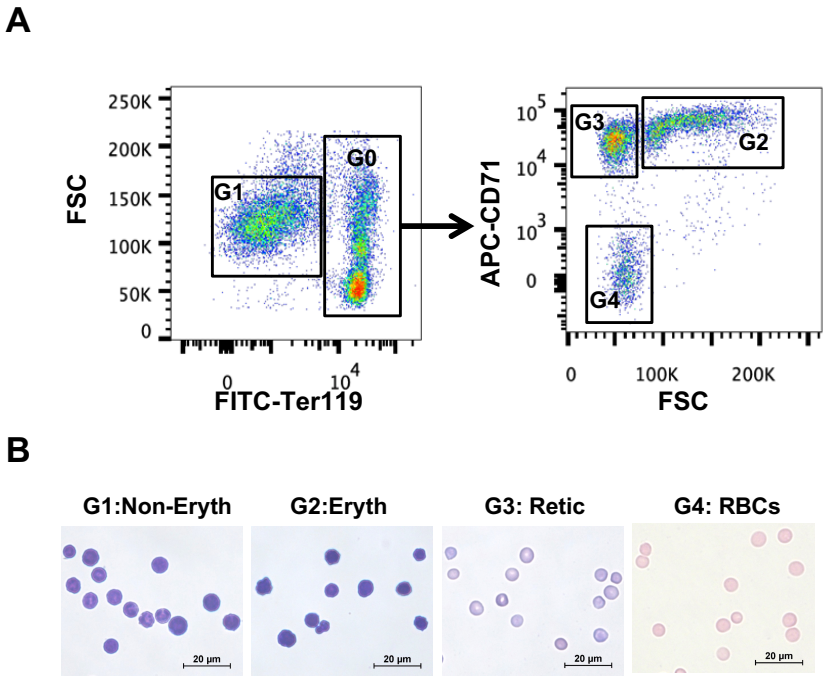

Figure S2. Flow cytometry to sort bone marrow cells into non-erythroblasts, erythroblasts, reticulocytes and RBCs. (**A**) Single viable cells were gated into non-erythroblasts (G1, Non-Eryth) and Ter119-positive erythroid cells (G0) that were further separated into erythroblasts (G2, Eryth), reticulocytes (G3, Retic) and mature RBCs (G4) according to the cell size (Forward scatter, FSC) and CD71 levels. (**B**) The purity of these four groups of cells was confirmed by May-Grünwald Giemsa staining.

Figure S3.

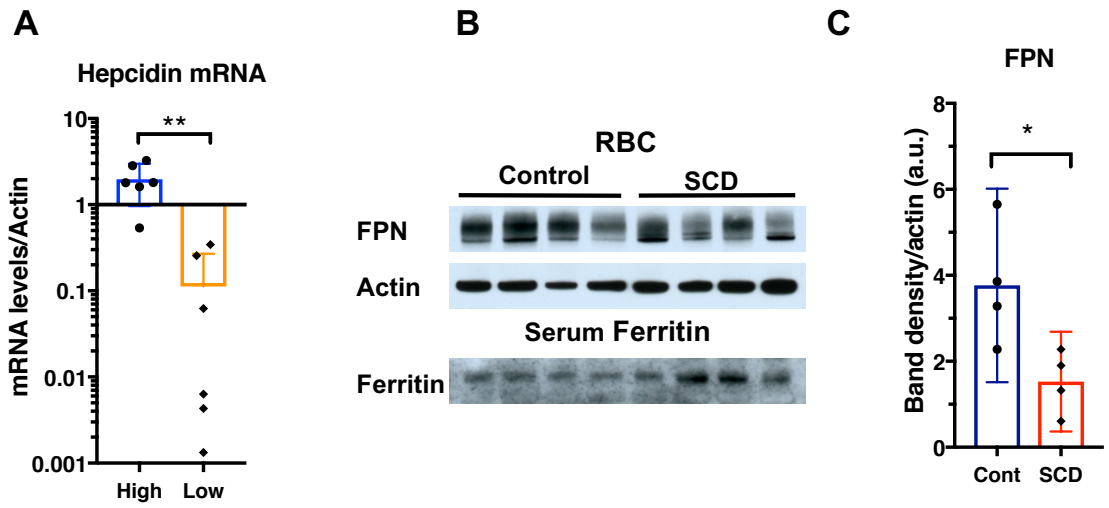

Figure S3. FPN abundance was inversely correlated with hepcidin levels. (**A**) Hepcidin mRNA levels in the livers of mice on high or low iron diets. Wild type mice were maintained on either a high iron or low iron diet for three months, and the hepcidin mRNA levels were measured with RT-PCR and normalized with actin mRNA levels. Statistical significance was determined with Welch's unequal variances t-test. (**B**) FPN levels were decreased in RBCs of sickle cell disease patients. (top) Immunoblots of FPN and actin in RBC ghost membranes of four control and four sickle cell disease (SCD) patients. (bottom) Immunoblots of ferritin in equal volumes of serum of control and SCD patients indicated that SCD patients were iron overloaded. **(C)** Analysis of FPN band intensity in panel B showed lower levels of FPN in RBCs of SCD patients. Since SCD patients had higher hepcidin levels *(*23), this results indicated that RBC FPN abundance inversely associated with hepcidin expression. The band intensities were measured by Adobe Photoshop, and normalized with actin. Data are presented as Mean ± 95% confidence interval in A and C.

Figure S4.

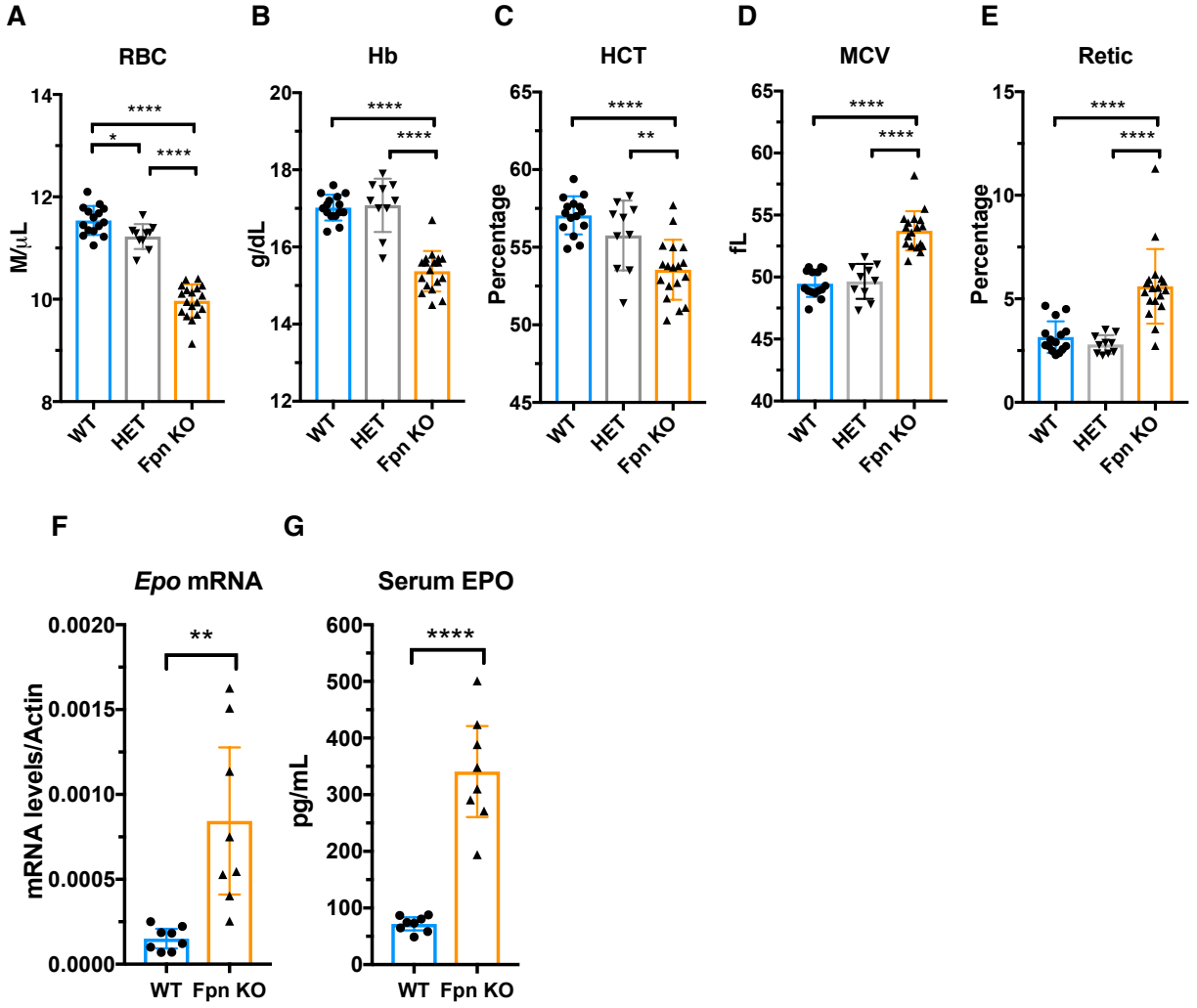

Figure S4. Cell-specific knockout of *Fpn* in erythroblasts caused compensated macrocytic anemia. (**A**) Red blood cell counts (RBC), (**B**) hemoglobin (Hb), (**C**) hematocrit (HCT), (**D**) mean corpuscular volume (MCV), and (**E**) reticulocytes (Retic) of WT, heterozygote (HET) and *Fpn* KO mice. Statistical significance was determined by one-way ANOVA and Tukey's multiple comparisons tests. (**F**) Erythropoietin (*Epo)* mRNA levels in kidneys and (**G**) serum EPO levels of WT and *Fpn* KO mice. *Fpn* KO mice had fewer RBCs, lower hemoglobins and hematocrits, along with increased mean corpuscular volumes (MCV) and EPO expression, doubled reticulocytes, indicating that FPN deficiency caused a compensated macrocytic anemia. Significance determined by Welch's t-test. Data are presented as Mean ± 95% confidence interval.

Figure S5.

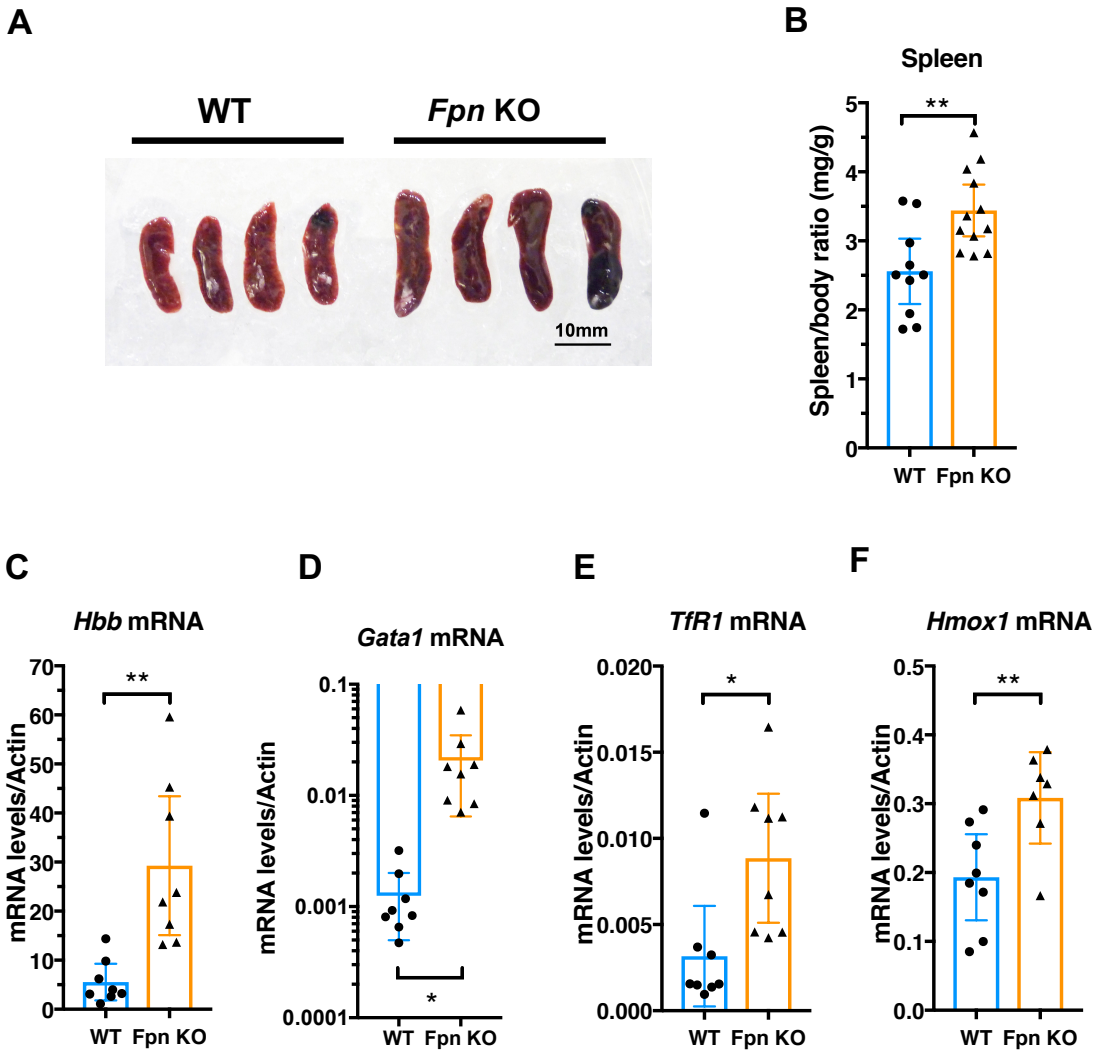

Figure S5. Cell-specific knockout of *Fpn* in erythroblasts caused splenomegaly and stress extramedullary erythropoiesis. (**A**) Representative pictures of spleens (Scale bar represents 10 mm) and (**B**) the spleen/body weight ratio of WT and *Fpn* KO mice. Compared to WT mice, the spleens of *Fpn* KO mice were darker and hypertrophic with average weights increased by 30%. **(C-F)** qRT-PCR analyses of splenic mRNA levels of (**C**) hemoglobin beta-chain (*Hbb*), (**D**) GATA-binding factor 1 (*Gata1)*, (**E**) transferrin receptor 1 (*TfR1)*, and (**F**) heme oxygenase 1 (*Hmox1)* indicated stress extramedullary erythropoiesis in *Fpn* KO mice. Panel D was analyzed with Welch's unequal variances t-test. Data are presented as mean ± 95% confidence interval.

Figure S6.

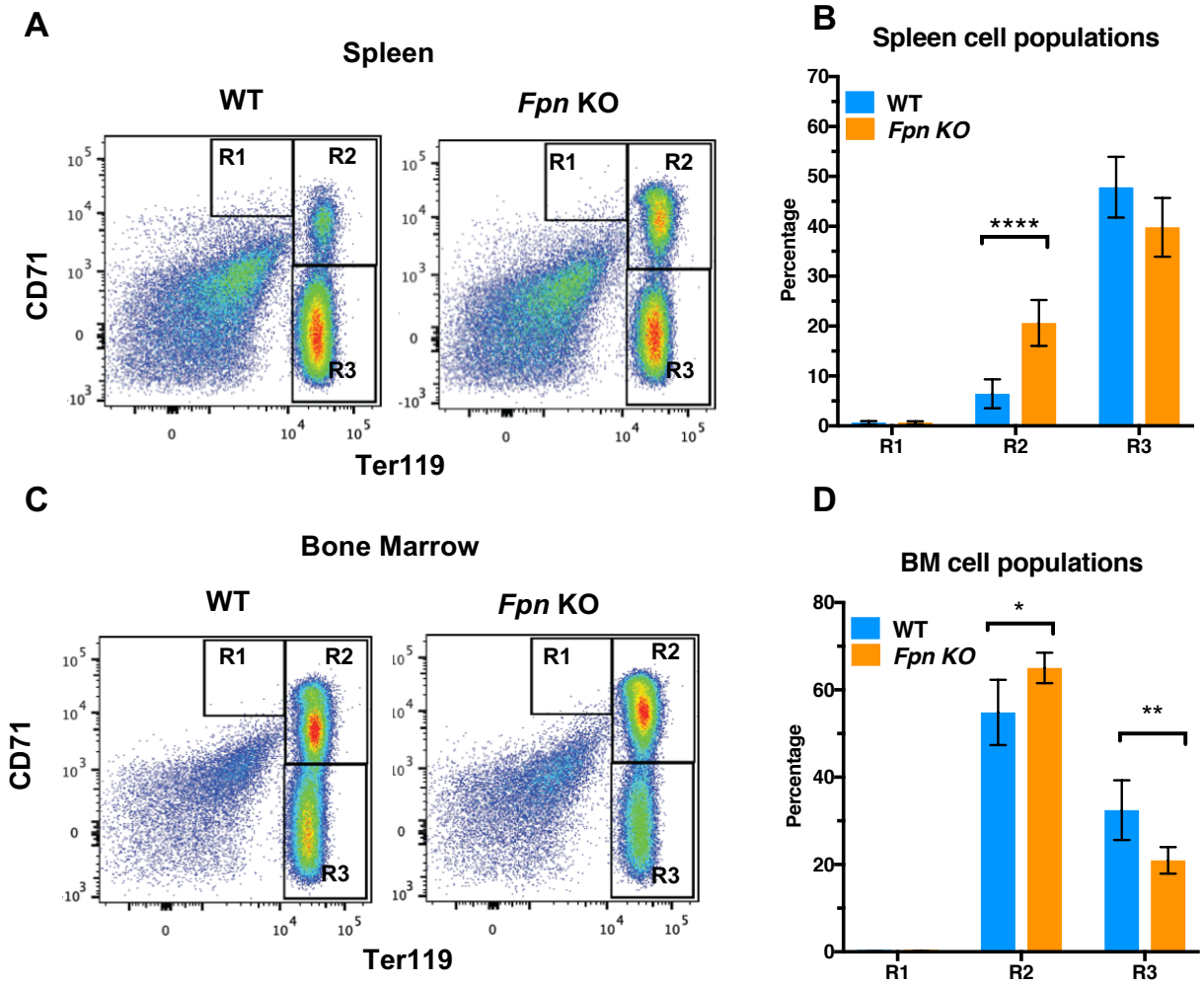

Figure S6. Analyses of cell populations in spleen and bone marrow showed stress erythropoiesis in *Fpn* KO mice. (**A, C**) Representative flow cytometry dot plots and (**B, D**) quantification of cell populations in spleen (**A, B**) and bone marrow (**C, D**) showed stress erythropoiesis. R1, proerythroblasts ($CD71^{high}Ter119^{low}$); R2, early erythroblasts ($CD71^{high}Ter119^{high}$); R3, later erythroblasts ($CD71^{low}Ter119^{high}$), mean ± 95% CI, n=9 for WT and n=12 for *Fpn* KO group; statistical significance determined using the Holm-Sidak method, with alpha = 0.05.

Figure S7.

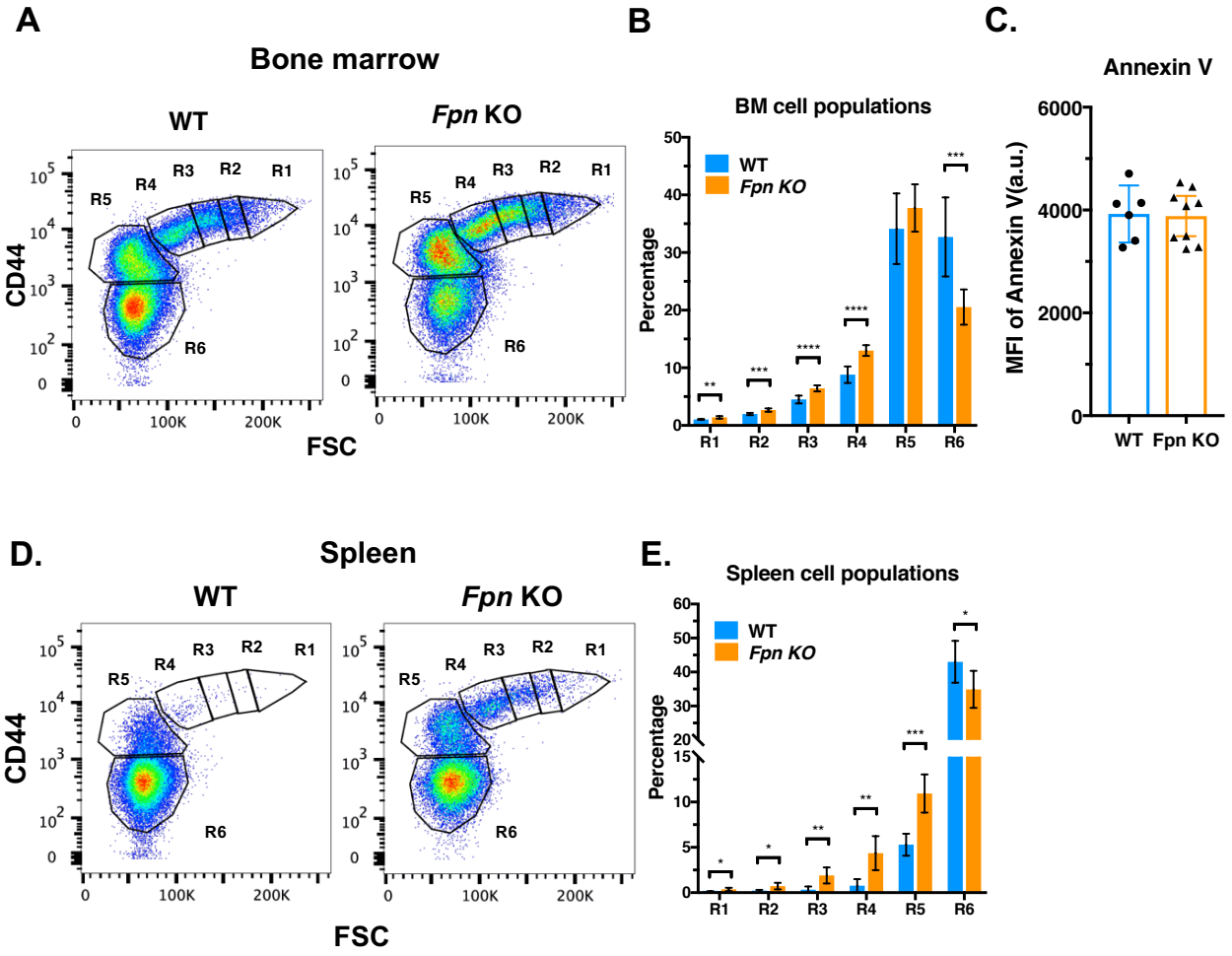

Figure S7. Cell population analyses showed normal differentiation of erythroblasts in *Fpn* KO mice. (**A, D**) Representative flow cytometry dot plots and (**B, E**) quantification of bone marrow **(A, B)** and **(D, E)** cells showed normal ratios between different stages of erythroblasts. (**C**) Annexin V staining of bone marrow erythroblasts of WT and *Fpn* KO mice. MFI, median fluorescence intensity; a.u., arbitrary unit. FSC, forward scatter, R1, proerythroblasts, R2, basophilic erythroblasts, R3, polychromatic erythroblasts, R4, orthochromatic erythroblasts, R5, reticulocytes, R6, mature RBCs. The ratios of R1:R2:R3:R4 were 1:2:4:8 in bone marrow (**A, B**) and spleen (**D, E**) of WT and *Fpn* KO mice, suggesting normal differentiation of erythroblasts. Data are presented as mean ± 95% confidence interval. (**B, E**) n=9 for WT and n=12 for *Fpn* KO group, statistical significance determined using the Holm-Sidak method with alpha = 0.05.

Figure S8.

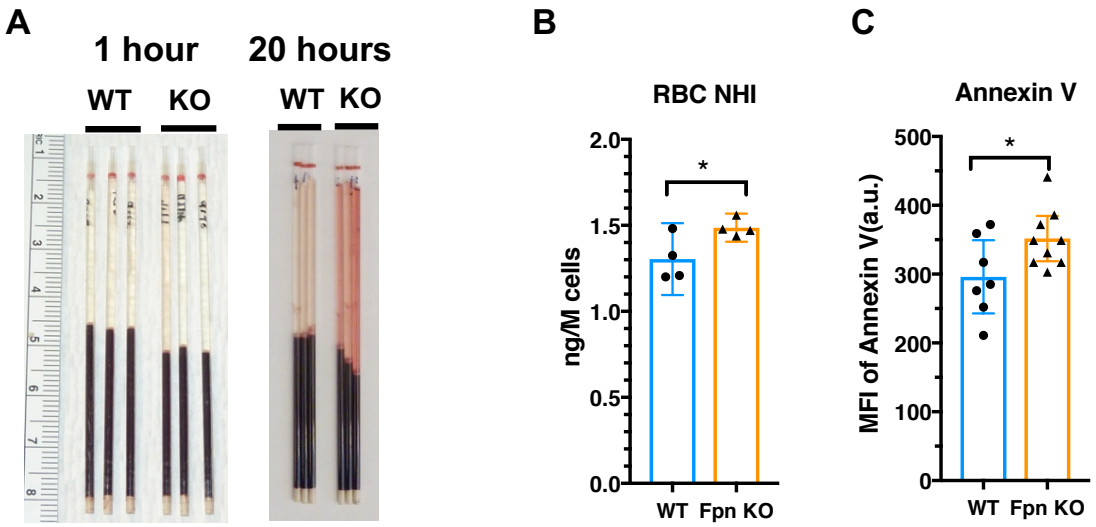

Figure S8. Hematocrits and spontaneous hemolysis of *Fpn* KO blood, and the increase of non-heme iron contents (NHI) and Annexin V staining in *Fpn* KO RBCs. (A) Representative pictures showed the blood of WT and *Fpn* KO in capillary tubes. The hematocrits of *Fpn* KO mice were significantly lower than WT mice. Plasmas of fresh blood of *Fpn* KO mice appeared normal, but turned red if the blood samples were stored at 4^{o}C for 20 hours, suggesting hemolysis. **(B)** Non-heme iron content (NHI) was significantly increased in *Fpn* KO RBCs. **(C)** Annexin V staining for RBCs of WT and *Fpn* KO mice. Data are presented as mean ± 95% confidence interval.

Figure S9.

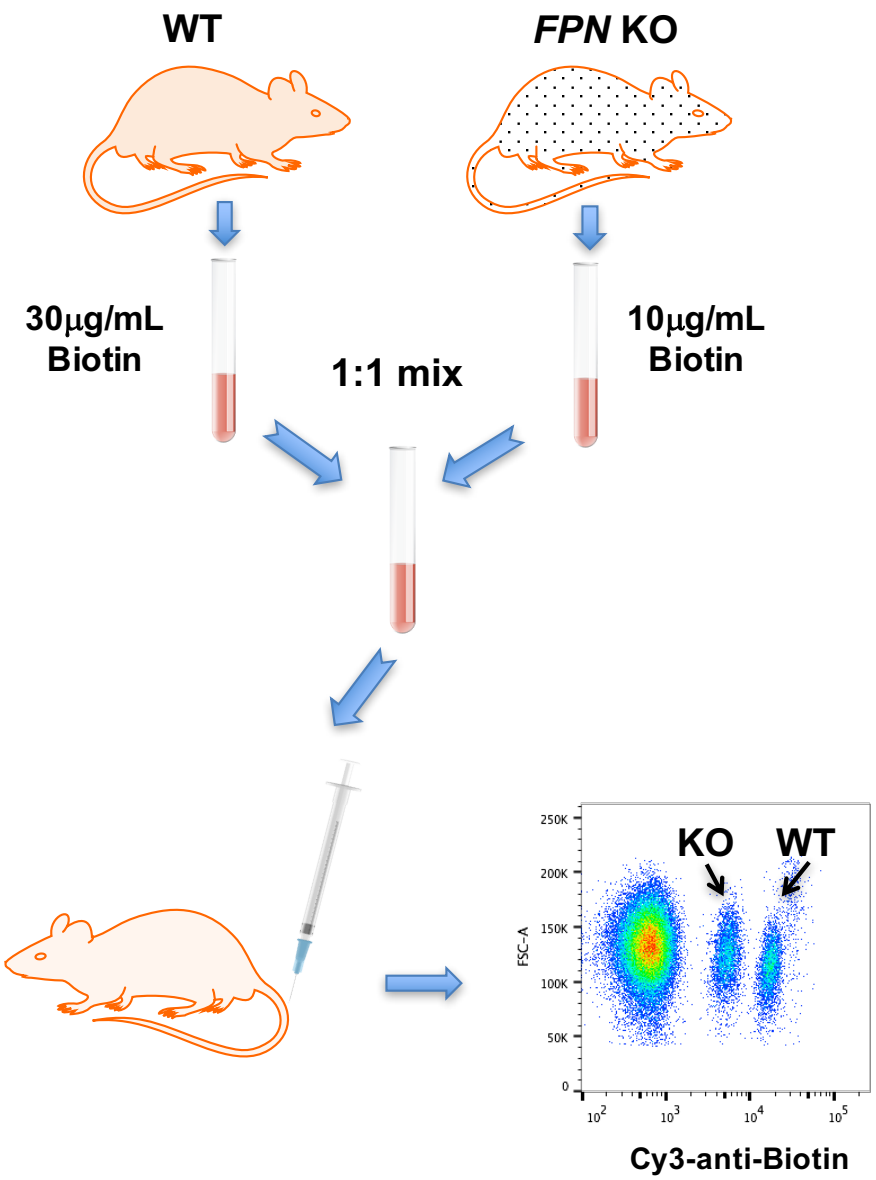

Figure S9. Strategy to measure autonomous defect of *Fpn* KO RBCs. Blood samples of WT and *Fpn* KO mice were washed with cold PBS for three times, then labeled with Sulfo-NHS-LC-Biotin (Biotin) 30 μg/mL for WT RBCs and 10 μg/mL for *Fpn* KO RBCs at 37°C for 30 min. After washing with PBS for three times, the blood samples were mixed in a 1:1 ratio and adjusted to 1x10e7 cells/μL, and then injected the mixture (300μL blood per mouse) via the tail vein into a WT mice. After 24 hours, 20 μL blood was collected and the percentage of Biotinylated RBCs was measured with Cy3-anti-Biotin antibody by a FACSAria flow cytometer. From the biotin levels, the RBCs of *Fpn* KO mice could be distinguished from WT RBCs and quantified.

Figure S10.

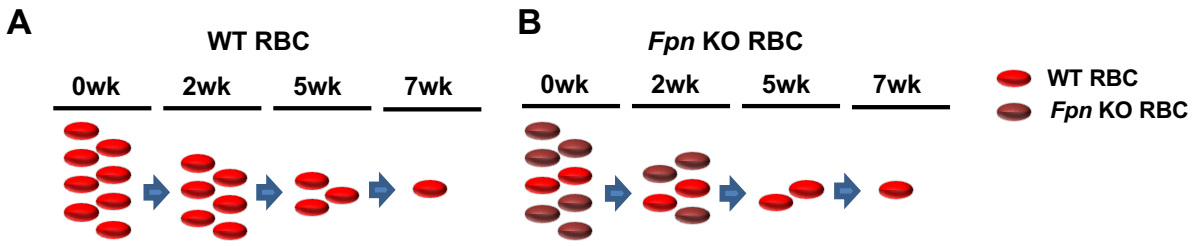

Figure S10. Schemes to explain why FPN levels apparently increased during RBC aging in *Fpn* conditional KO mice (Fig. 2J). In the erythroblast-specific *Fpn* KO mice, there were a few FPN-expressing RBCs (WT RBC) remained, as indicated by the faint band in *Fpn* KO RBCs (Fig. 1B). The very few residual FPN-expressing RBCs (WT RBC) had longer lifespans than *Fpn-null* RBCs *(Fpn* KO RBC*)* and consequently survived and were enriched during the aging process, indicating that FPN-expressing RBCs had a survival advantage *in vivo*.

Figure S11.

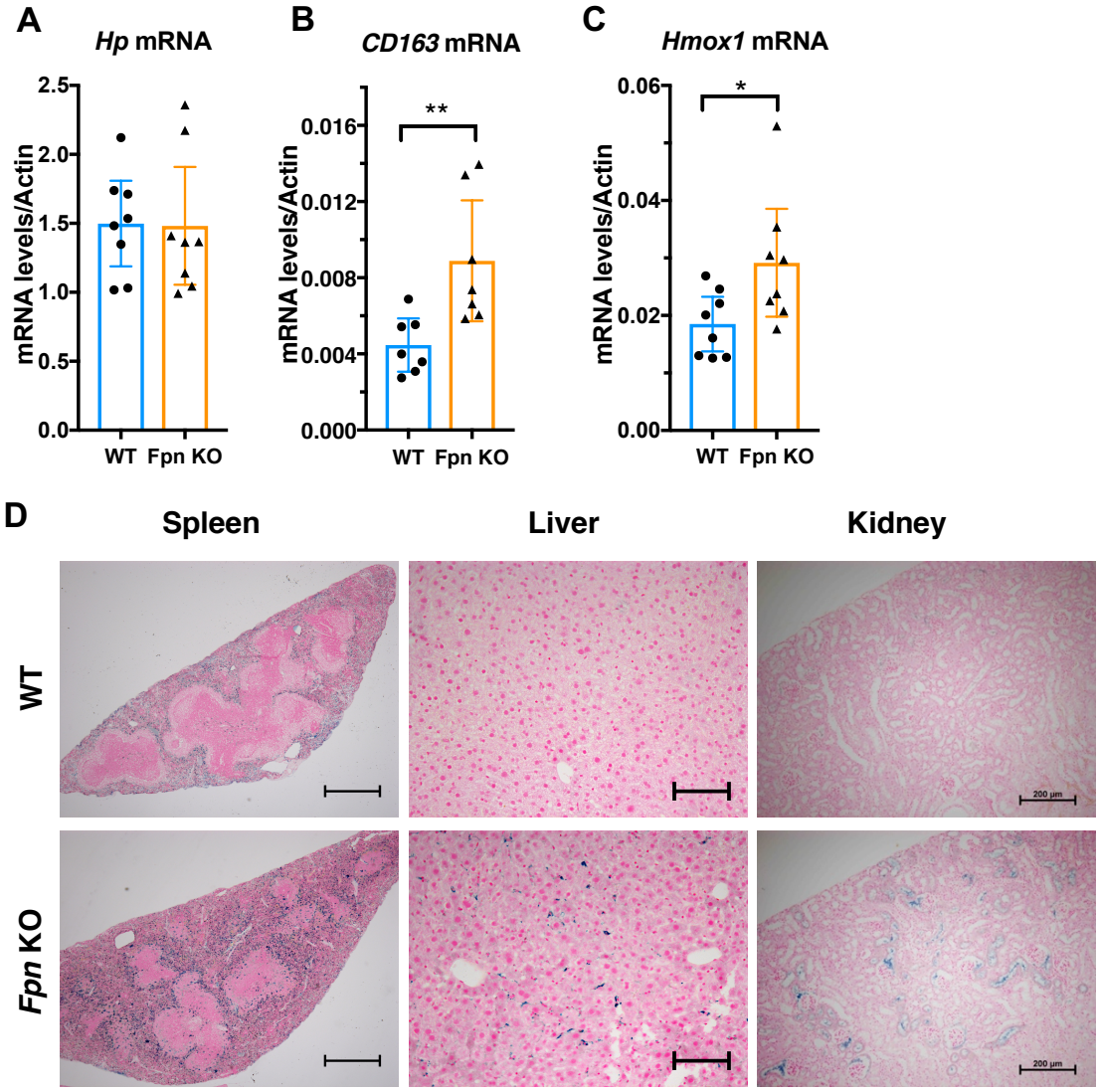

Figure S11. mRNA expression in livers of WT and *Fpn* KO mice and Prussian blue iron staining of spleen, liver and kidney. The mRNA levels of (**A)** haptoglobin (*Hp*), (**B**) *CD163,* and (**C**) *Hmox1* (heme oxygenase 1) in livers of WT and *Fpn* KO mice. Data are presented as mean ± 95% confidence interval. **(D)** *Fpn* deficiency in erythroid cells caused iron overload in splenic macrophages, hepatic Kupffer cells and renal proximal tubules. Representative Prussian blue iron staining of spleen, liver and kidneys of WT and *Fpn* KO mice. As shown in the figures, iron (Blue staining) was dramatically accumulated in splenic macrophages, hepatic Kupffer cells, and renal proximal tubules. Bars represent 500 μm for spleen, 200 μm for kidney and 100 μm for liver. Increased *CD163* and *Hmox1* expression, iron accumulation in splenic macrophages, hepatic Kupffer cells and renal proximal tubules, along with serum haptoglobin depletion (Fig. 1K) and increased reticulocytosis (fig. S4E) indicated that *Fpn* KO mice suffered from hemolytic anemia.

Figure S12.

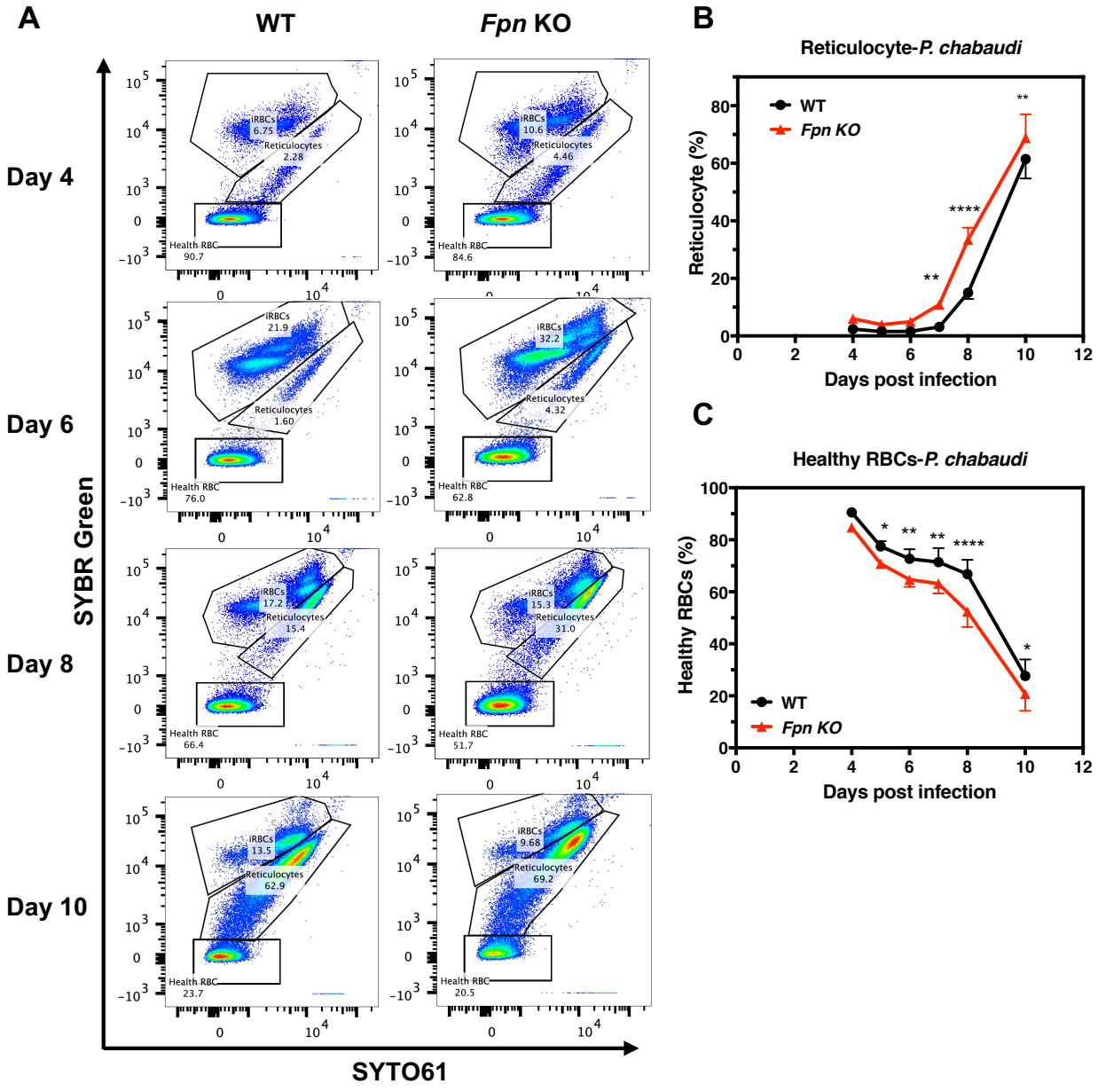
A
WT
Fpn KO
Day 4
Day 6
Day 8
Day 10
SYBR Green
SYTO61
iRBCs
6.75
Reticulocytes
2.28
Health RBC
90.7
iRBCs
10.6
Reticulocytes
4.46
Health RBC
84.6
iRBCs
21.9
Reticulocytes
1.60
Health RBC
76.0
iRBCs
32.2
Reticulocytes
4.32
Health RBC
62.8
iRBCs
17.2
Reticulocytes
15.4
Health RBC
66.4
iRBCs
15.3
Reticulocytes
31.0
Health RBC
51.7
iRBCs
13.5
Reticulocytes
62.9
Health RBC
23.7
iRBCs
9.68
Reticulocytes
69.2
Health RBC
20.5
B
Reticulocyte-P. chabaudi
WT
Fpn KO
Reticulocyte (%)
Days post infection
C
Healthy RBCs-P. chabaudi
WT
Fpn KO
Healthy RBCs (%)
Days post infection

Figure S12. The changes of parasitemia, reticulocyte counts and healthy RBCs in WT and *Fpn* KO mice on successive days after infection by *Plasmodium chabaudi*. (**A**) Representative flow cytometry dot plots of blood of WT or *Fpn* KO mice on different days after infection by *Plasmodium chabaudi chabaudi AS.* Changes of (**B**) reticulocytes and (**C**) healthy RBCs in WT and *Fpn* KO mice after infection by *Plasmodium chabaudi.* WT or *Fpn* KO mice were infected by *P. chabaudi,* and blood samples were collected at indicated times and analyzed with flow cytometry after staining with SYBR Green and SYTO61. The populations of infected RBCs (iRBCs), reticulocytes and healthy mature RBCs were indicated as in the plots. Notably, *P. chabaudi* parasites did not infect reticulocytes. Numbers of infected RBCs were higher in *Fpn* KO mice than in WT mice on days 4 and 6, but numbers of infected cells diminished as the proportion of reticulocytes increased and healthy cells decreased. Mean ± 95% CI, n=5 for WT and n=7 for *Fpn* KO mice, statistical significance determined with two-way ANOVA and Sidak's multiple comparisons tests.

Figure S13.

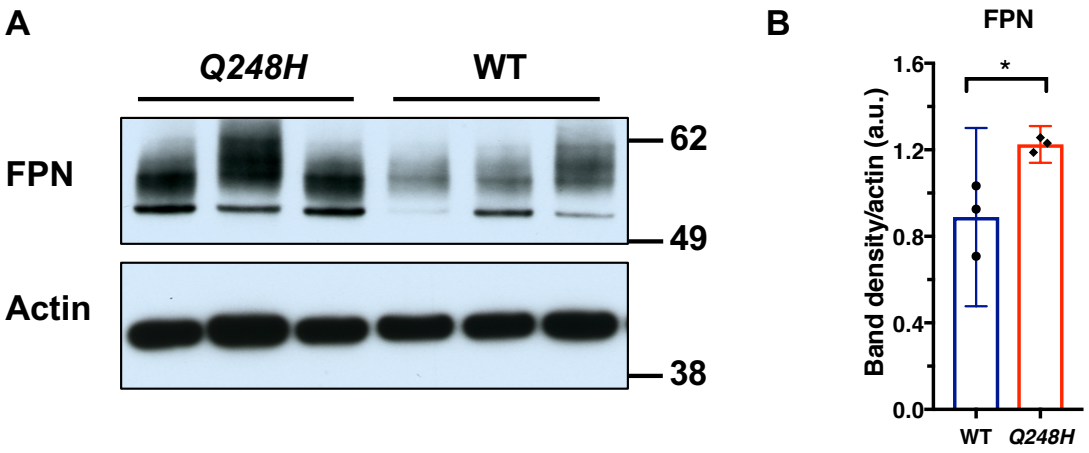

Figure S13. FPN protein abundance was significantly increased in the RBCs of *FPN Q248H* heterozygote blood donors. (A) Immunoblot analysis of FPN protein abundance in RBC membrane fractions of three wild type (WT) and three *FPN Q248H* heterozygote blood donors. Actin was used as loading control. **(B)** Analysis of FPN band density in panel A showed higher levels of FPN in RBCs of *Q248H* heterozygote compared to WT. The band intensities were measured by Adobe Photoshop, and normalized with actin. Mean ± 95% CI, a.u., arbitrary unit.

Figure S14.

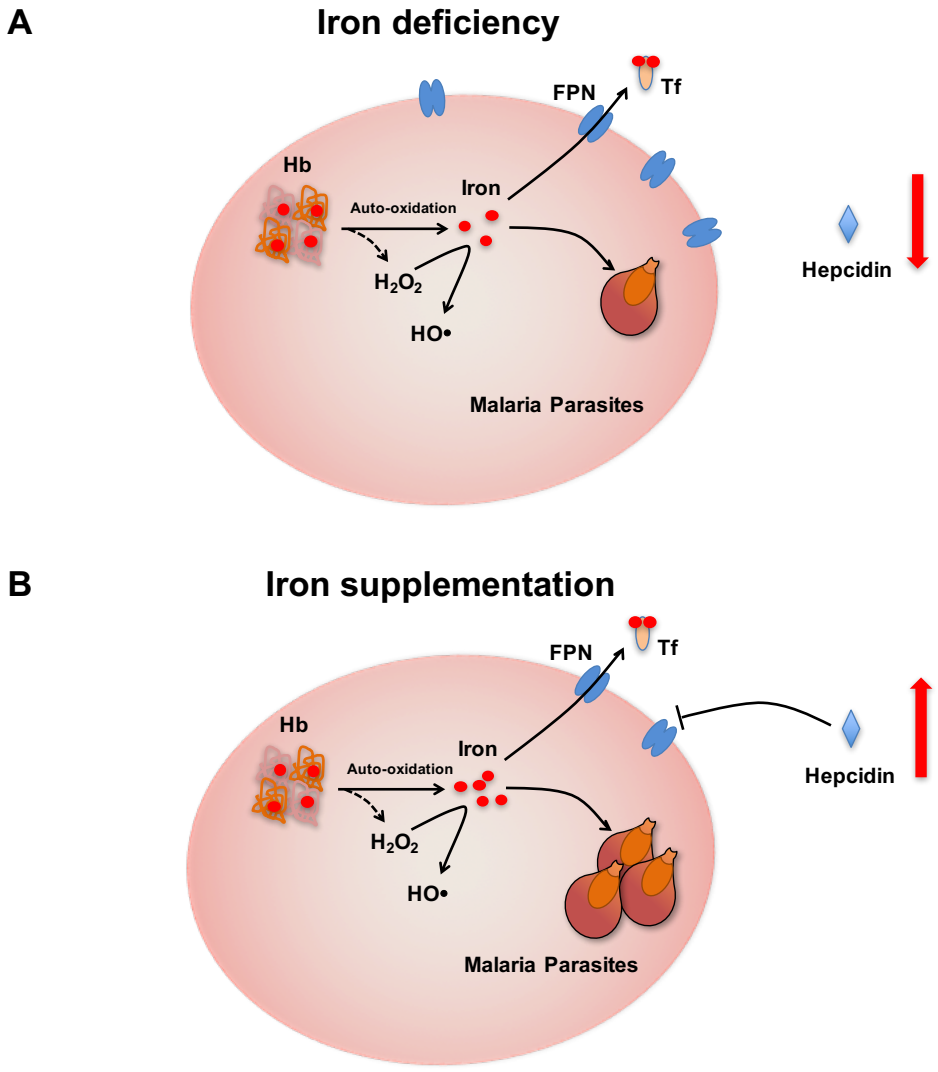

Figure S14. Scheme of the function of FPN on RBCs and during malaria infection. (A) FPN is highly abundant on mature RBCs, from which it exports free iron that is generated during auto-oxidation of hemoglobin and thereby prevents iron-mediated oxidative stress. By removing free intracellular iron, FPN inhibits the growth and proliferation of malarial parasites. **(B)** Upon iron supplementation, hepcidin levels increase. Hepcidin induces the degradation of FPN on erythroblasts, which leads to diminished levels of FPN on mature RBCs; also, hepcidin directly inhibits the activity of FPN on RBCs, leading to increased intracellular iron that promotes malarial growth. Hb, hemoglobin; Tf, transferrin.

Note: Table S1 is a separate file in Excel format.

Table S1. Mass spectrum analysis of the protein abundance in RBC membrane fractions. The mass spectrum data for red cell membrane were reported by *Pesciotta* and her colleagues in their previous publication (*22*), and were downloaded from the Peptide Atlas data repository with the dataset identifier PASS00334 (www.peptideatlas.org). The data were analyzed with Excel, and the number of peptides identified for each protein was summarized and listed accordingly. The abundance of Band 3 was taken as 1000,000 copies per cell (*46*), and the rest of the proteins were normalized with Band 3 and ordered accordingly. The proteins listed in Table 1 were highlighted in red. Noticeably, the copy number of FPN in RBCs of Diamond Blackfan Anemia patients was lower than that of control group. Considering that DBA patients were reported to have high hepcidin levels (*22*), this result indicated that RBC FPN levels inversely correlated with hepcidin expression.

Table S2.

Table S2. Blood indices of WT, heterozygote and *Fpn* KO mice

Hematological Parameters of 8-12 weeks old mice			
Parameter	*FPN*$^{fl/fl}$*ErCre*$^{-/-}$ (WT, n=15)	*FPN*$^{fl/+}$*ErCre*$^{+/-}$ (Het, n=11)	*FPN*$^{fl/fl}$*ErCre*$^{+/-}$ (KO, n=17)
RBC ($10^6/\mu L$)	11.54±0.16	11.23±0.18 *	9.97±0.16 ****, aaaa
Hb (g/dL)	17.02±0.18	17.08±0.49	15.37±0.26****, aaaa
HCT (%)	52.60±0.58	51.50±1.18	47.72±0.65 ****, aaaa
MCV (fL)	49.46±0.59	49.65±1.01	53.73±0.78 ****, aaaa
MCH (pg)	14.75±0.19	15.20±0.37 *	15.43±0.20 ****
MCHC (g/dL)	29.83±0.14	30.62±0.46 ****	28.71±0.18 ****, aaaa
RET (%)	3.15±0.42	2.80±0.33	5.61±0.89 ****, aaaa

RBC, red blood cell; Hb, hemoglobin; HCT, hematocrit; MCV, mean corpuscular volume; MCH, mean corpuscular hemoglobin; MCHC, mean corpuscular hemoglobin content; RET, reticulocyte. Data are reported as mean ± 95% confidence interval, significance determined by one-way ANOVA with Tukey's multiple comparisons test. vs. WT, * p<0.05, ****p<0.0001; vs. Het, aaaa p<0.0001.

Fpn KO mice had fewer RBCs, lower hemoglobins and hematocrits, along with increased mean corpuscular volumes (MCV) and mean corpuscular hemoglobin (MCH), and doubled reticulocytes, indicating that FPN deficiency caused a compensated macrocytic anemia. Notably, there were no dramatic hematological differences between wild type (WT) and heterozygotes, confirming that the anemia was specifically caused by homozygous FPN deficiency.

Table S3

Table S3. Zambian children admitted to hospital with uncomplicated malaria

	All (N = 66)	Wildtype (N = 53)	*FPN Q248H* (N = 13)	P
Demographic and history				
Age, months (median and IQ range)	29 (18-37)	29 (17-37)	34 (26-42)	0.16
Male gender, %	50% (33/66)	47.2% (25/53)	61.5% (8/13)	0.54
Antimalarial treatment before presenting, %	36.4% (24/66)	35.8% (20/53)	38.5% (5/13)	1.00
Traditional herbal medicine before presenting, %	22.7% (15/66)	24.5% (13/53)	15.4% (2/13)	0.72
Physical examination				
Temperature, Deg C (median and IQ range)	37.8 (36.8-38.7)	37.8 (36.5-38.6)	37.6 (37.2-39.4)	0.39
Weight, kg (median and IQ range)	10.8 (8.9-12.6)	10.4 (8.8-12.4)	12.3 (10.8-13.6)	0.12
Weight for age z-score (median and IQ range)	-1.6 (-2.2 - -0.9)	-1.6 (-2.7 - -0.9)	-1.6 (-2.0 - -0.8)	0.70
Spleen, cm below costal margin (median and IQ range)	1 (0-2)	1 (0-2)	0 (0-1)	0.15
Liver, cm below costal margin (median and IQ range)	0 (0-1)	0 (0-1)	0 (0-2)	0.96
Laboratory tests				
Mean corpuscular volume, fL (median and IQ range)	70 (63-76)	70 (64-77)	68 (61-75)	0.59
Reticulocytes, % (median and IQ range)	1.2 (0.7-2.0)	1.1 (0.6-2.0)	1.4 (1.0-1.9)	0.36
Platelets, x $10^3/\mu L$ (median and IQ range)	112 (74-171)	116 (74-166)	91 (71-188)	0.95
White blood cells, x$10^3/\mu L$ (median and IQ range)	7.8 (5.7-11.1)	7.7 (5.3-10.8)	8.8 (6.6-14.0)	0.17

The *FPN Q248H* mutation was observed in 19.7% of the children (12 heterozygous, 1 homozygous), and genotype frequencies were in Hardy-Weinberg equilibrium (χ^2=0.11, p=0.74). In addition, infected *Q248H* carriers appeared to remain sufficiently healthy to endure additional cycles of parasitemia and hemolysis before presenting to the hospital. Consistent with the latter point is that after adjustment for the duration of fever, the mean hemoglobin concentrations were only slightly lower in the *Q248H* patients (9.2±0.7 vs. 9.5±0.3 g/dL, *Q248H* vs. control, p=0.7) (See Table 2). Categorical variables were compared with the Fisher exact test and continuous variables were compared with the Kruskal-Wallis test.

Table S4.

Table S4. Ghanaian primiparous women, live singleton delivery, *n* = 290

	All N = 290	Wildtype N = 265	*FPN Q248H* N = 25	P
General findings				
Age (years, mean ± SD)	21.3 ± 3.5	21.3 ± 3.5	21.2 ± 3.4	0.87
Residence in Agogo	50.0 (145/290)	49.8 (132/265)	52.0 (13/25)	0.83
Delivery in rainy season	53.1 (154/290)	54.0 (143/265)	44.0 (11/25)	0.34
Pyrimethamine in plasma (chemoprophylaxis)	35.8 (102/285)	35.6 (93/261)	37.5 (9/24)	0.86
>3 antenatal care visits	52.7 (149/283)	51.9 (134/258)	60.0 (15/25)	0.44
Caesarian section	22.1 (64/290)	21.5 (57/265)	28.0 (7/25)	0.45
Peripheral blood findings				
Microscopy positive	26.6 (77/290)	27.2 (72/265)	20.0 (5/25)	0.44
GMPD (/µL; 95%CI), n = 73	793 (502-1251)	718 (446-1154)	3034 (926-9940)	0.12
HRP2 dipstick positive	44.8 (130/290)	45.3 (120/265)	40.0 (10/25)	0.61
PCR positive	59.0 (171/290)	60.4 (160/265)	44.0 (11/25)	0.11
Placental blood findings				
Microscopy positive	45.5 (132/290)	46.4 (123/265)	36.0 (9/25)	0.32
GMPD (95%CI;/100 HPF), n=132	117 (75-181)	106 (68-166)	408 (55-3006)	0.13
Hemozoin (pigment) positive	42.1 (122/290)	43.0 (114/265)	32.0 (8/25)	0.29
HRP2 dipstick positive	50.2 (145/289)	50.8 (134/264)	44.0 (11/25)	0.52
PCR positive	64.8 (188/290)	66.8 (177/265)	44.0 (11/25)	0.03
Any positive placental finding*	67.9 (197/290)	70.2 (186/265)	44.0 (11/25)	0.007
Clinical findings				
Hemoglobin (g/dL; mean ± SD)	11.24 ± 1.8	11.21 ± 1.87	11.46 ± 1.54	0.52
Anemia (Hb<11 g/dL)	37.9 (110/290)	38.9 (103/265)	28.0 (7/25)	0.28
Birth weight (g; median, range)	2795 (1280-4000)	2800 (1280-4000)	2770 (1500-3800)	0.80
Low birth weight (<2500 g)	26.2 (76/290)	25.7 (68/265)	32.0 (8/25)	0.49
Gestational age (weeks; mean ± SD)	38.1 ± 2.6	38.1 ± 2.6	38.0 ± 2.4	0.90
Preterm delivery (<37 weeks)	26.6 (77/290)	26.4 (70/265)	28.0 (7/25)	0.86
Fever (>37.4°C, axillary)	4.2 (12/287)	4.2 (11/262)	4.0 (1/25)	0.96

Table S4.

Data are given as % (n/n) unless otherwise stated. GMPD, geometric mean parasite density; HPF, high power field, SD, standard deviation. Proportions were compared between groups by Chi-square test, and continuous variables by Student´s t-test or Mann Whitney U test (birth weight). Genotype frequencies were consistent with the Hardy-Weinberg equilibrium ($\chi 2$=0.33, p=0.57). * Present or past placental *P. falciparum* infection, defined as the microscopic detection of placental parasitemia or hemozoin, the malaria pigment, or a positive PCR result on placental blood samples. It occurred less frequently in *Q248H* carriers than in women with the respective wildtype allele (odds ratio, 0.33; 95%CI, 0.13-0.82; p=0.007). After adjusting by logistic regression for known predictors of placental malaria in this group (*39*), the association of *Q248H* carriage with reduced odds of present or past placental *P. falciparum* infection remained significant (adjusted odds ratio [aOR], 0.31; 95%CI, 0.13-0.75; p=0.009; age (years), aOR, 0.91; 95%CI, 0.84-0.98; rainy season, aOR, 1.74; 95%CI, 1.03-2.92; pyrimethamine in plasma (reflecting chemoprophylaxis), aOR, 0.64, 95%CI, 0.38-1.09).
No significant effect of *FPN Q248H* on clinical outcomes (anemia, LBW, preterm delivery) after stratification by infection status. No significant interaction between *FPN Q248H* and infection status on clinical outcomes (ANOVA). No significant impact of *FPN Q248H* on PCV, MCV, RBC. Anemia appeared to be slightly less common in *Q248H* carriers than in WT women but no significant differences in peripheral and placental parasite densities, birth weight, or preterm delivery were seen. Only 4.2% of the women were febrile despite a prevalence of placental malaria of 67.9%, in consistence with malaria in pregnancy frequently being asymptomatic in areas of high endemicity.

Table S5.

Table S5. Primers for qRT-PCR

Primers for qRT-PCR		
Gene	**Primer F**	**Primer R**
Fpn	ATGGGAACTGTGGCCTTCAC	TCCAGGCATGAATACGGAGA
Epo	AGGAGGCAGAAAATGTCACG	CCACCTCCATTCTTTTCCAA
Hbb	ATGGCCTGAATCACTTGGAC	ACGATCATATTGCCCAGGAG
Gata1	ATGGCAAGACGGCACTCTAC	TCAAGGTGTCCAAGAACGTG
TfR1	TTGCGGCGAAGTCCAGTGTG	CCTGCAGTCCAGCTGGCAAA
Hmox1	GGTACACATCCAAGCCGAGA	TCCAGGGCCGTGTAGATATG
Hp	CAACTGTTGGGAATTGCACTGCG	ACGAAGTAGTCACGGGCATCCAG
Hepcidin	TTGCGATACCAATGCAGAAG	TGCAACAGATACCACACTGG
CD163	TGTGCAGTGTCCAAAAGGAG	TGTATGCCCTTCCTGGAGTC
Actin	GCCACTGCCGCATCCTCTTC	AGCCTCAGGGCATCGGAACC

References

1. A. F. Cowman, J. Healer, D. Marapana, K. Marsh, Malaria: Biology and disease. *Cell* **167**, 610–624 (2016). doi:10.1016/j.cell.2016.07.055 Medline
2. P. A. Sigala, J. R. Crowley, S. Hsieh, J. P. Henderson, D. E. Goldberg, Direct tests of enzymatic heme degradation by the malaria parasite *Plasmodium falciparum*. *J. Biol. Chem.* **287**, 37793–37807 (2012). doi:10.1074/jbc.M112.414078 Medline
3. M. A. Clark, M. M. Goheen, C. Cerami, Influence of host iron status on *Plasmodium falciparum* infection. *Front. Pharmacol.* **5**, 84 (2014). doi:10.3389/fphar.2014.00084 Medline
4. P. F. Scholl, A. K. Tripathi, D. J. Sullivan, Bioavailable iron and heme metabolism in *Plasmodium falciparum*. *Curr. Top. Microbiol. Immunol.* **295**, 293–324 (2005). doi:10.1007/3-540-29088-5_12 Medline
5. A. M. Prentice, Iron metabolism, malaria, and other infections: What is all the fuss about? *J. Nutr.* **138**, 2537–2541 (2008). doi:10.3945/jn.108.098806 Medline
6. J. M. Rifkind, E. Nagababu, S. Ramasamy, L. B. Ravi, Hemoglobin redox reactions and oxidative stress. *Redox Rep.* **8**, 234–237 (2003). doi:10.1179/135100003225002817 Medline
7. J. Umbreit, Methemoglobin—It's not just blue: A concise review. *Am. J. Hematol.* **82**, 134–144 (2007). doi:10.1002/ajh.20738 Medline
8. T. Kanias, J. P. Acker, Biopreservation of red blood cells—The struggle with hemoglobin oxidation. *FEBS J.* **277**, 343–356 (2010). doi:10.1111/j.1742-4658.2009.07472.x Medline
9. S. Sazawal, R. E. Black, M. Ramsan, H. M. Chwaya, R. J. Stoltzfus, A. Dutta, U. Dhingra, I. Kabole, S. Deb, M. K. Othman, F. M. Kabole, Effects of routine prophylactic supplementation with iron and folic acid on admission to hospital and mortality in preschool children in a high malaria transmission setting: Community-based, randomised, placebo-controlled trial. *Lancet* **367**, 133–143 (2006). doi:10.1016/S0140-6736(06)67962-2 Medline
10. M. Gwamaka, J. D. Kurtis, B. E. Sorensen, S. Holte, R. Morrison, T. K. Mutabingwa, M. Fried, P. E. Duffy, Iron deficiency protects against severe *Plasmodium falciparum* malaria and death in young children. *Clin. Infect. Dis.* **54**, 1137–1144 (2012). doi:10.1093/cid/cis010 Medline
11. N. Spottiswoode, P. E. Duffy, H. Drakesmith, Iron, anemia and hepcidin in malaria. *Front. Pharmacol.* **5**, 125 (2014). doi:10.3389/fphar.2014.00125 Medline

12. D. L. Zhang, M. C. Ghosh, T. A. Rouault, The physiological functions of iron regulatory proteins in iron homeostasis—An update. *Front. Pharmacol.* **5**, 124 (2014). doi:10.3389/fphar.2014.00124 Medline
13. N. Wilkinson, K. Pantopoulos, The IRP/IRE system in vivo: Insights from mouse models. *Front. Pharmacol.* **5**, 176 (2014). doi:10.3389/fphar.2014.00176 Medline
14. A. Donovan, C. A. Lima, J. L. Pinkus, G. S. Pinkus, L. I. Zon, S. Robine, N. C. Andrews, The iron exporter ferroportin/Slc40a1 is essential for iron homeostasis. *Cell Metab.* **1**, 191–200 (2005). doi:10.1016/j.cmet.2005.01.003 Medline
15. H. Drakesmith, E. Nemeth, T. Ganz, Ironing out ferroportin. *Cell Metab.* **22**, 777–787 (2015). doi:10.1016/j.cmet.2015.09.006 Medline
16. S. Abboud, D. J. Haile, A novel mammalian iron-regulated protein involved in intracellular iron metabolism. *J. Biol. Chem.* **275**, 19906–19912 (2000). doi:10.1074/jbc.M000713200 Medline
17. E. Nemeth, M. S. Tuttle, J. Powelson, M. B. Vaughn, A. Donovan, D. M. Ward, T. Ganz, J. Kaplan, Hepcidin regulates cellular iron efflux by binding to ferroportin and inducing its internalization. *Science* **306**, 2090–2093 (2004). doi:10.1126/science.1104742 Medline
18. D. L. Zhang, R. M. Hughes, H. Ollivierre-Wilson, M. C. Ghosh, T. A. Rouault, A ferroportin transcript that lacks an iron-responsive element enables duodenal and erythroid precursor cells to evade translational repression. *Cell Metab.* **9**, 461–473 (2009). doi:10.1016/j.cmet.2009.03.006 Medline
19. D. L. Zhang, T. Senecal, M. C. Ghosh, H. Ollivierre-Wilson, T. Tu, T. A. Rouault, Hepcidin regulates ferroportin expression and intracellular iron homeostasis of erythroblasts. *Blood* **118**, 2868–2877 (2011). doi:10.1182/blood-2011-01-330241 Medline
20. A. C. Heinrich, R. Pelanda, U. Klingmüller, A mouse model for visualization and conditional mutations in the erythroid lineage. *Blood* **104**, 659–666 (2004). doi:10.1182/blood-2003-05-1442 Medline
21. E. N. Pesciotta, S. Sriswasdi, H.-Y. Tang, D. W. Speicher, P. J. Mason, M. Bessler, Dysferlin and other non-red cell proteins accumulate in the red cell membrane of Diamond-Blackfan anemia patients. *PLOS ONE* **9**, e85504 (2014). doi:10.1371/journal.pone.0085504 Medline
22. D. Pospisilova, D. Holub, Z. Zidova, L. Sulovska, J. Houda, V. Mihal, I. Hadacova, L. Radova, P. Dzubak, M. Hajduch, V. Divoky, M. Horvathova, Hepcidin levels in Diamond-Blackfan anemia reflect erythropoietic activity and transfusion

dependency. *Haematologica* **99**, e118–e121 (2014). doi:10.3324/haematol.2014.104034 Medline

23. Z. A. Jenkins, W. Hagar, C. L. Bowlus, H. E. Johansson, P. Harmatz, E. P. Vichinsky, E. C. Theil, Iron homeostasis during transfusional iron overload in beta-thalassemia and sickle cell disease: Changes in iron regulatory protein, hepcidin, and ferritin expression. *Pediatr. Hematol. Oncol.* **24**, 237–243 (2007). doi:10.1080/08880010701360700 Medline
24. R. Taniguchi, H. E. Kato, J. Font, C. N. Deshpande, M. Wada, K. Ito, R. Ishitani, M. Jormakka, O. Nureki, Outward- and inward-facing structures of a putative bacterial transition-metal transporter with homology to ferroportin. *Nat. Commun.* **6**, 8545 (2015). doi:10.1038/ncomms9545 Medline
25. S. Aschemeyer, B. Qiao, D. Stefanova, E. V. Valore, A. C. Sek, T. A. Ruwe, K. R. Vieth, G. Jung, C. Casu, S. Rivella, M. Jormakka, B. Mackenzie, T. Ganz, E. Nemeth, Structure-function analysis of ferroportin defines the binding site and an alternative mechanism of action of hepcidin. *Blood* **131**, 899–910 (2018). doi:10.1182/blood-2017-05-786590 Medline
26. K. Schümann, N. W. Solomons, Can iron supplementation be reconciled with benefits and risks in areas hyperendemic for malaria? *Food Nutr. Bull.* **34**, 349–356 (2013). doi:10.1177/156482651303400307 Medline
27. I. Kasvosve, Z. A. R. Gomo, K. J. Nathoo, P. Matibe, B. Mudenge, M. Loyevsky, V. R. Gordeuk, Effect of ferroportin Q248H polymorphism on iron status in African children. *Am. J. Clin. Nutr.* **82**, 1102–1106 (2005). doi:10.1093/ajcn/82.5.1102 Medline
28. D. Albuquerque, L. Manco, K. M. Loua, A. P. Arez, Mde. J. Trovoada, L. Relvas, T. S. Millimono, S. L. Rath, D. Lopes, F. Nogueira, L. Varandas, M. Alvarez, M. L. Ribeiro, *SLC40A1* Q248H allele frequencies and associated *SLC40A1* haplotypes in three West African population samples. *Ann. Hum. Biol.* **38**, 378–381 (2011). doi:10.3109/03014460.2010.541496 Medline
29. V. R. Gordeuk, A. Caleffi, E. Corradini, F. Ferrara, R. A. Jones, O. Castro, O. Onyekwere, R. Kittles, E. Pignatti, G. Montosi, C. Garuti, I. T. Gangaidzo, Z. A. R. Gomo, V. M. Moyo, T. A. Rouault, P. MacPhail, A. Pietrangelo, Iron overload in Africans and African-Americans and a common mutation in the *SCL40A1* (ferroportin 1) gene. *Blood Cells Mol. Dis.* **31**, 299–304 (2003). doi:10.1016/S1079-9796(03)00164-5 Medline
30. S. Nekhai, M. Xu, A. Foster, I. Kasvosve, S. Diaz, R. F. Machado, O. L. Castro, G. J. Kato, J. G. Taylor VI, V. R. Gordeuk, Reduced sensitivity of the ferroportin

Q248H mutant to physiological concentrations of hepcidin. *Haematologica* **98**, 455–463 (2013). doi:10.3324/haematol.2012.066530 Medline

31. M. E. Molyneux, T. E. Taylor, J. J. Wirima, A. Borgstein, Clinical features and prognostic indicators in paediatric cerebral malaria: A study of 131 comatose Malawian children. *Q. J. Med.* **71**, 441–459 (1989). Medline
32. P. E. Thuma, J. van Dijk, R. Bucala, Z. Debebe, S. Nekhai, T. Kuddo, M. Nouraie, G. Weiss, V. R. Gordeuk, Distinct clinical and immunologic profiles in severe malarial anemia and cerebral malaria in Zambia. *J. Infect. Dis.* **203**, 211–219 (2011). doi:10.1093/infdis/jiq041 Medline
33. M. Fried, F. Nosten, A. Brockman, B. J. Brabin, P. E. Duffy, Maternal antibodies block malaria. *Nature* **395**, 851–852 (1998). doi:10.1038/27570 Medline
34. M. A. Grundy, N. Gorman, P. R. Sinclair, M. J. Chorney, G. S. Gerhard, High-throughput non-heme iron assay for animal tissues. *J. Biochem. Biophys. Methods* **59**, 195–200 (2004). doi:10.1016/j.jbbm.2004.01.001 Medline
35. M. J. Murray, A. B. Murray, M. B. Murray, C. J. Murray, The adverse effect of iron repletion on the course of certain infections. *BMJ* **2**, 1113–1115 (1978). doi:10.1136/bmj.2.6145.1113 Medline
36. J. Liu, J. Zhang, Y. Ginzburg, H. Li, F. Xue, L. De Franceschi, J. A. Chasis, N. Mohandas, X. An, Quantitative analysis of murine terminal erythroid differentiation in vivo: Novel method to study normal and disordered erythropoiesis. *Blood* **121**, e43–e49 (2013). doi:10.1182/blood-2012-09-456079 Medline
37. F. P. Mockenhaupt, G. Bedu-Addo, C. von Gaertner, R. Boyé, K. Fricke, I. Hannibal, F. Karakaya, M. Schaller, U. Ulmen, P. A. Acquah, E. Dietz, T. A. Eggelte, U. Bienzle, Detection and clinical manifestation of placental malaria in southern Ghana. *Malar. J.* **5**, 119 (2006). doi:10.1186/1475-2875-5-119 Medline
38. G. Snounou, S. Viriyakosol, X. P. Zhu, W. Jarra, L. Pinheiro, V. E. do Rosario, S. Thaithong, K. N. Brown, High sensitivity of detection of human malaria parasites by the use of nested polymerase chain reaction. *Mol. Biochem. Parasitol.* **61**, 315–320 (1993). doi:10.1016/0166-6851(93)90077-B Medline
39. C. A. Rivers, J. C. Barton, V. R. Gordeuk, R. T. Acton, M. R. Speechley, B. M. Snively, C. Leiendecker-Foster, R. D. Press, P. C. Adams, G. D. McLaren, F. W. Dawkins, C. E. McLaren, D. M. Reboussin, Association of ferroportin Q248H polymorphism with elevated levels of serum ferritin in African Americans in the Hemochromatosis and Iron Overload Screening (HEIRS) study. *Blood Cells Mol. Dis.* **38**, 247–252 (2007). doi:10.1016/j.bcmd.2006.12.002 Medline

40. D. Darbari, M. Loyevsky, V. Gordeuk, J. A. Kark, O. Castro, S. Rana, V. Apprey, J. Kurantsin-Mills, Fluorescence measurements of the labile iron pool of sickle erythrocytes. *Blood* **102**, 357–364 (2003). doi:10.1182/blood-2002-03-0914 Medline
41. S. Wang, G. L. Dale, P. Song, B. Viollet, M. H. Zou, AMPKα1 deletion shortens erythrocyte life span in mice. *J. Biol. Chem.* **285**, 19976–19985 (2010). doi:10.1074/jbc.M110.102467 Medline
42. D. M. Mock, N. I. Matthews, S. Zhu, R. G. Strauss, R. L. Schmidt, D. Nalbant, G. A. Cress, J. A. Widness, Red blood cell (RBC) survival determined in humans using RBCs labeled at multiple biotin densities. *Transfusion* **51**, 1047–1057 (2011). doi:10.1111/j.1537-2995.2010.02926.x Medline
43. G. Hoffmann-Fezer, J. Mysliwietz, W. Mörtlbauer, H. J. Zeitler, E. Eberle, U. Hönle, S. Thierfelder, Biotin labeling as an alternative nonradioactive approach to determination of red cell survival. *Ann. Hematol.* **67**, 81–87 (1993). doi:10.1007/BF01788131 Medline
44. J. Poole, Red cell antigens on band 3 and glycophorin A. *Blood Rev.* **14**, 31–43 (2000). doi:10.1054/blre.1999.0124 Medline
45. L. J. Wu, A. G. M. Leenders, S. Cooperman, E. Meyron-Holtz, S. Smith, W. Land, R. Y. L. Tsai, U. V. Berger, Z.-H. Sheng, T. A. Rouault, Expression of the iron transporter ferroportin in synaptic vesicles and the blood-brain barrier. *Brain Res.* **1001**, 108–117 (2004). doi:10.1016/j.brainres.2003.10.066 Medline
46. M. C. Ghosh, W.-H. Tong, D. Zhang, H. Ollivierre-Wilson, A. Singh, M. C. Krishna, J. B. Mitchell, T. A. Rouault, Tempol-mediated activation of latent iron regulatory protein activity prevents symptoms of neurodegenerative disease in IRP2 knockout mice. *Proc. Natl. Acad. Sci. U.S.A.* **105**, 12028–12033 (2008). doi:10.1073/pnas.0805361105 Medline
47. T. L. Steck, J. A. Kant, Preparation of impermeable ghosts and inside-out vesicles from human erythrocyte membranes. *Methods Enzymol.* **31**, 172–180 (1974). doi:10.1016/0076-6879(74)31019-1 Medline